Grating Assisted Coupling in Microring Resonators

A. Samarelli, M. Sorel, R.M. De La Rue
Electronic and Electrical Department,
Glasow University,
Glasgow, United Kingdom
antonios@elec.gla.ac.uk

A. Melloni
Dipartimento di Elettronica e Informazione,
Politecnico di Milano
Milano, Italy

P. Orlandi, M. Gnan, P.Bassi
Dipartimento di Elettronica, Informatica e Sistemistica,
Università di Bologna
Bologna, Italy

Abstract—**Grating Assisted Couplers (GACs) in Silicon-on-Insulator waveguides are studied experimentally as building blocks for optical integrated devices. By including them in a microring resonator configuration, we enhance the GAC wavelength selectivity and limit the resonance range of the microring. This device has the potential for small footprint, highly selective, wavelength filters and sensors.**

Keywords-grating assisted coupler; microring resonator; silicon-on-insulator;

I. INTRODUCTION

Silicon-on-insulator (SOI) technology is a promising platform for constructing functional micro-scale optical devices for high-density photonic integration. Among the various unit elements that can be developed as building blocks for SOI photonic circuits, the Grating Assisted Coupler (GAC) can perform optical routing among different waveguides while being highly wavelength selective. GACs have been realized in $LiNbO_3$ [1], optical fibers [2], and, recently, also in SOI [3]. If they are designed to operate on nanometer sized bandwidths (e.g. for applications such as WDM add-drop filters or sensors) the grating is weak, resulting in many hundreds of micrometre long devices [3]. In this paper, after demonstrating the coupling properties of weak sidewall GACs in SOI, we show numerically and experimentally that a GAC in a microring resonator configuration takes advantage of the optical feedback to reduce both its coupling bandwidth and device footprint.

II. GRATING ASSISTED COUPLER

A GAC consists of two waveguides placed side by side where a common grating mediates the coupling between the modes of the waveguides (Fig. 1). When two counter-propagating modes belonging to the same waveguide are coupled, their Bragg condition is $\beta_i = \pi/\Lambda$, where *i* specifies the waveguide, Λ is the grating period, and β_i is the propagation constant. When two modes of different waveguides are involved, the Bragg condition is $\beta_i + \beta_j = 2\pi/\Lambda$, which is halfway between the two previous coupling regimes. If the grating is sufficiently weak, the Coupled Mode Theory (CMT) approach can be used. Furthermore, the three coupling regimes can be modeled separately if they are sufficiently spaced in wavelength [4]. In order to use GACs as building blocks for optical devices, we have studied the properties of a set of GACs fabricated in SOI, made out of waveguides having weak sidewall modulation.

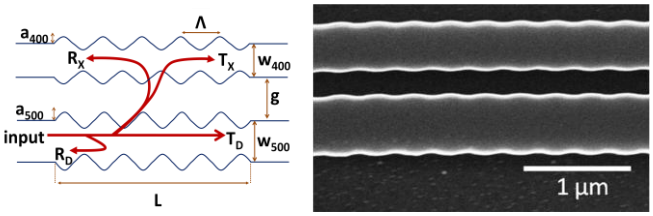

Figure 1 Schematic and micrograph of fabricated GAC.

A 220-nm silicon core layer on a 1-μm buried oxide sample of SOI wafer from SOITEC was patterned using electron beam lithography and HSQ resist – and subsequently dry-etched [5]. Inverse tapers coupled to polymer SU8 waveguides were used to terminate all the silicon waveguides so as to minimize back reflection at the waveguide ends and improve the coupling efficiency. The fabricated devices were finally embedded in 900 nm of oxide formed as a bi-layer of HSQ and deposited SiO_2.

The waveguides of the GACs were 500 nm and 400 nm wide, providing different propagation constants in single modal regimes with low propagation losses [5]. Each sidewall has a sinusoidal modulation with an amplitude parameter *a*. The wider waveguide has a larger modulation so that $a_{500} > a_{400}$. The average gap between the two waveguides is *g* and the length of the coupling region is *L*.

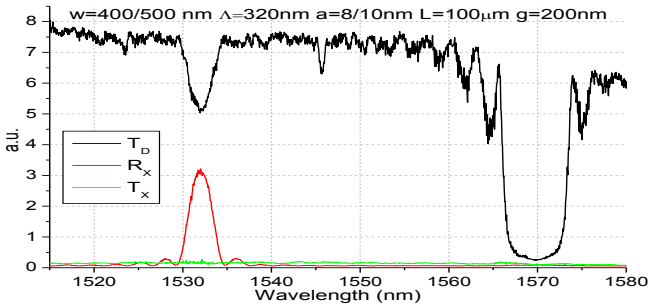

Figure 2 – Experimental transmission of GAC (dimensions specified in figure heading)

Fig. 2 shows experimental direct transmission (T_D), cross transmission (T_X), and cross reflection (R_X) curves of a GAC with Λ = 320 nm, a_{400} = 8 nm, a_{500} = 10 nm, L = 100 μm g = 200 nm. The right-most stop-band shape in T_D (centered at λ~1570 nm) is the direct stop-band of the feeder 500 nm wide waveguide. The left-most stop-band (at $\lambda_0 \sim 1532$ nm) is the exchange coupling stop-band, where direct transmission drops in favor of cross-reflected power (R_X). The "missing" other direct stop-band (at λ_0~1494 nm, according to CMT) would be

visible if the input power were inserted into the 400 nm wide waveguide. The cross-transmission is always isolated from the feeder waveguide. The weak modulation of the transmittance is presumably due to residual co-directional coupling.

The experimental cross-coupling coefficients of various geometrical configurations obtained varying the sidewall modulation amplitude (*a*), gap (*g*) are shown in Table 1.

a_{400} / a_{500} → g ↓	4nm / 6nm	8nm / 10 nm	10nm / 15 nm
200 nm	0.00397±0.00005	0.0062 ± 0.0002	0.0074 ± 0.0002
220 nm	0.003± 0.00008	0.0049 ± 0.0005	0.0072 ± 0.0004
240 nm	0.0025±0.0002	0.0043 ± 0.0006	0.0048 ± 0.0003

Table 1 Experimental exchange coupling coefficients (units are μm^{-1})

The very small value of the exchange coupling coefficients is closely related to the nanometre sized bandwidth of the exchange stop-band shown in Fig. 2. Because of the weak coupling factors, large exchange reflections can only be obtained by hundreds of micrometres of propagation, which would result in too large a device footprint. In the next section, we propose a configuration where the length of the device can be kept short by using the optical feedback of a microring resonator configuration.

III. GAC IN MICRORING CONFIGURATION

The schematic of the microring resonator with two GAC elements is shown in Fig. 3. ASPIC software [6] with transfer matrix and CMT methods was used to simulate the device behavior. Fig. 4 shows results with Λ = 320 nm, a_{400} = 10 nm, a_{500} = 15 nm, L = 20.16 µm, g = 220 nm, and coupling coefficients as detailed in Table 1. The input and output waveguides are 400 nm wide, while the ring waveguide is 500 nm wide with a 20 µm radius.

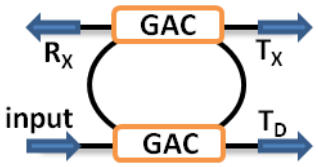

Figure 3 Sketch of the microring resonator with GAC elements.

Besides the direct stop-band of the feeder waveguide, the main feature of the simulated behavior is the set of ring resonance dips limited to the exchange coupling bandwidth of the GACs. From the point of view of the GACs, the optical resonance of the ring enhances its effective length, thus making it more wavelength selective. We believe that this device can be tailored so as to allow only the set of wavelengths that are needed, for example, in WDM filters or sensing devices. The simulated device was then fabricated and its measured characteristics are shown in Fig. 5. On the whole, the curves reproduce the simulated ones very closely. The main difference is found in the fact that the cross-transmission (T_X) is as large as the cross-reflection (R_X). This can be explained by spurious reflections within the resonator, possibly at the interface between the grating and the feedback wires – or by roughness-induced backscatter.

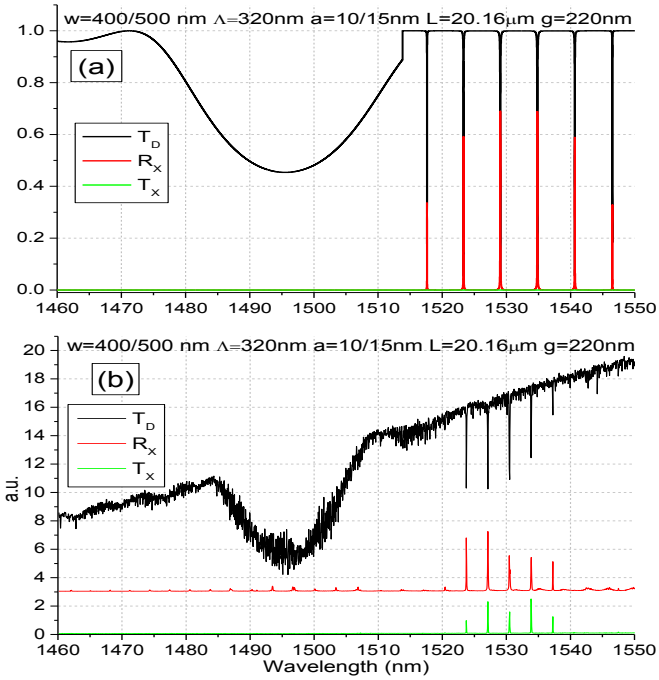

Figure 4 (a) Simulated and (b) experimental behavior of GAC in microring configuration. Note that R_x has been offset by 3 for readability.

IV. CONCLUSION AND FUTURE WORK

The experimental behavior of sidewall GACs fabricated in SOI with various geometries was demonstrated. By arranging two GACs in a microring resonator configuration we have demonstrated numerically and experimentally, enhancement of the selectivity of the GAC or, conversely, the limitation of the resonance of the microring resonator. This device has the potential to be tailored to become a highly wavelength selective add-drop filter or sensor – while maintaining a compact footprint.

ACKNOWLEDGMENT

We thank the JWNC staff at GU for support in fabrication of the devices and Gaetano Bellanca for helpful discussions. We acknowledge SPLASH and PROMINER projects for funding.

REFERENCES

[1] P. Yeh and H.F. Taylor, "Contradirectional frequency-selective couplers for guided-wave optics," Appl. Optics, vol. 19, pp. 2848-2855, 1980.

[2] S. Orlov, A. Yariv, and S. Van Essen, "Coupled-mode analysis of fiber-optic add drop filters for dense wavelength-division multiplexing," Opt. Lett., vol. 22, pp. 688-690, 1997.

[3] D.H. Tan, K. Ikeda, and Y. Fainman, "Coupled chirped vertical gratings for on-chip group velocity dispersion engineering," Appl. Phys. Lett., vol. 95, p. 141109, 2009.

[4] R. Syms, "Optical directional coupler with a grating overlay," Appl. Optics, vol. 24, pp. 717-726, 1985.

[5] M. Gnan, S. Thoms, D. Macintyre, R. De La Rue, and M. Sorel, "Fabrication of low-loss photonic wires in silicon-on-insulator using hydrogen silsesquioxane electron-beam resist," Electron. Lett., vol. 44, pp. 44-45, 2008.

[6] ASPIC Design. Filarete, Italy, 2009 – website www.aspicdesign.com